POLITECNICO DI TORINO
Repository ISTITUZIONALE

Determining the Particle Size of Debris from a Tunnel Boring Machine Through Photographic Analysis and Comparison Between Excavation Performance and Rock Mass

Original
Determining the Particle Size of Debris from a Tunnel Boring Machine Through Photographic Analysis and Comparison Between Excavation Performance and Rock Mass Properties / Rispoli, A.; Ferrero, A. M.; Cardu, Marilena; Farinetti, A.. - In: ROCK MECHANICS AND ROCK ENGINEERING. - ISSN 0723-2632. - STAMPA. - 50:(2017), pp. 2805-2816. [10.1007/s00603-017-1256-5]

Availability:
This version is available at: 11583/2676746 since: 2017-10-10T13:48:48Z

Publisher:
Springer-Verlag Wien

Published
DOI:10.1007/s00603-017-1256-5

Terms of use:

This article is made available under terms and conditions as specified in the corresponding bibliographic description in the repository

Publisher copyright
Springer postprint/Author's Accepted Manuscript

This version of the article has been accepted for publication, after peer review (when applicable) and is subject to Springer Nature's AM terms of use, but is not the Version of Record and does not reflect post-acceptance improvements, or any corrections. The Version of Record is available online at: http://dx.doi.org/10.1007/s00603-017-1256-5

(Article begins on next page)

06 May 2026

Determining the particle size of the TBM's debris through photographic analysis and comparison between excavation performance and rock mass properties

A. Rispoli & A.M. Ferrero
Earth Sciences Department, Università degli Studi di Torino, Italy
M. Cardu
DIATI-Politecnico di Torino; IGAG-CNR, Torino, Italy

Abstract
The paper presents the results of a study carried out on a 6.3 m diameter exploratory tunnel excavated in hard rock by an open TBM. The study provides a methodology, based on photographic analysis, for the evaluation of the particle size distribution of debris produced by TBM. A number of tests was carried out on the debris collected during the TBM advancement; to provide a parameter indicative of the particle size of the debris, the coarseness index CI was defined, and compared with some parameters representative of the TBM performance, i.e. the excavation specific energy SE and the field penetration index FPI, and with the rock-mass features, such as RMR, GSI and uniaxial compression strength. The results obtained showed a clear trend between CI and some TBM performance parameters, such as SE and FPI; on the contrary, due to the rock mass fracturing, a clear relationship between CI and rock mass characteristics was not found.

Keywords: Debris size distribution, Photographic analysis, Field Specific Energy, Coarseness Index, TBM performance, Hard Rock TBM

Introduction

Excavation by TBM in hard rock-like environments is by now the most commonly adopted technique in tunnel projects longer than 1 km, because of the considerable advantages gained both in terms of time and development costs. The successful use of this technique goes through the proper design of the cutterhead, which is strongly dependent on the characteristics of the material under excavation.
TBM performance are thus conditioned by finding, during excavation, conditions similar to those provided at the design stage; for these reasons, to evaluate the efficiency of the excavation, the performance evaluation cannot disregard the definition of the actual conditions of the rock mass. In this regard, the particle size of the debris produced during excavation is able to give information on both cutting efficiency and characteristics of the rock mass. In fact, numerous studies have examined the relationship between the size of the debris particles and some of the machine's performance indicators (e.g. Roxborough and Rispin, 1973; McFeat-Smith and Fowell, 1977; Altindag, 2003; Tuncdemir et al., 2008; Balci, 2009; Abu Bakar et al., 2014). In particular, it is known as the specific energy, indicator of the efficiency of the excavation and defined as the energy needed to excavate a unit volume of rock, assumes, for a given rock and type of tool, a decreasing trend with increasing the particle size obtained from the rock fragmentation process; this condition is especially detectable in the laboratory (Roxborough and Rispin, 1973) but also on site, as evidenced by the results obtained from Tundemir et al. (2008). Farrokh & Rostami (2008) and Balci (2009) have also found that the presence of discontinuities and other structural features in the rock influence the debris size.
The systematic assessment on site of the particle size obtained in a TBM excavation, however, is not simple: the particle size distribution of the debris is in fact normally very wide. The theory of the rock breaking mechanism through disc tools involves the detachment of rock chips together with pulverized and granular rock; Gertsch et al. (2000) notice how the chips size depends on the disc

tools spacing as well as on the penetration value taken during each revolution of the cutterhead; however, in fractured rock mass conditions, the particle sizes of the debris can be significantly larger because of the displacement of rock blocks due to the presence of crossing joints (Farrokh & Rostami, 2008). For these reasons, the particle size distribution of the debris may provide both pulverized rock and fragments whose dimensions can reach several tens of centimeters. In these conditions, to regularly apply the traditional classification method by sieving (coarse part) and sedimentation (fine part) several problems would be involved: first, not being able to use sieves for the analysis of blocks with decimetric dimensions, it would be necessary to manually measure each fragment by means of a series of screens; moreover, being the representative volume to analyze for each sampling dependent on the maximum size of the fragments, it would result considerably high, i.e. at least 40 kg for a maximum size of 63 mm (BS EN 933-1, 2012), and a comprehensive analysis would thus require a very long time. Finally, the debris collected to perform the sieving test, to be highly representative, should be taken directly from the conveyor belt, as suggested by Bruland (1998), and this condition would affect the excavation cycle, being not recommended to stop the belt before its downloading.
To face the above problems, the present study proposes a methodology for the analysis of the debris from TBM through photographic analysis. This method, previously adopted by Rispoli et al. (2016), allows to quickly analyze a large volume of debris (about 3 m^3 for each sampling), with contained costs: it does not need an analysis laboratory and requires little labor (both the sampling and the processing phases may be carried out by one operator). The method, due to its simplicity, is systematically implementable (on a daily basis, together with the other investigations carried out during the progress of TBM) and not interferes with the excavation cycle, since the sample is taken from the piles of debris outside the tunnel. The proposed method is essentially based on the determination of the 3D volumes of debris through the processing of images appropriately taken from isolated portions of the piles. For this purpose, the *Split Desktop 3.1* software, distributed by *Split Engineering LLC* (www.spliteng.com) was employed. It allows the evaluation of the particle size distribution of the portion of debris analyzed; however, whereas the coarse fraction is determined by the direct assessment of the fragments observed on the image, the finer part is the result of a statistical estimation: for these reasons, it has been chosen to detail only the coarse part of the samples analyzed (size greater than about 10 mm). In this regard, Farrokh & Rostami (2008) correlated the tunnel convergence with the size distribution of the muck estimated by visual observation of rock fragments in the muck cars; they did not analyze the particle size distribution of the fragments smaller than 2 cm, and claimed that the portion of debris with sizes between 2 and 10 cm represents the ground conditions where the face is stable and is actually being excavated.
The results proposed in this study are based on a campaign analysis carried out in the *Maddalena* exploratory tunnel, excavated with a 6.3 m diameter TBM while crossing the *Clarea* complex, mainly characterized by mica-schists and with RMR between 41 and 80 .

The results related to the particle size distribution of the debris will be both compared with some parameters representative of the TBM performance, i.e. the excavation specific energy and the field penetration index, and with the rock-mass features, in terms of RMR, GSI and uniaxial compression strength. In particular, in order to provide a parameter indicative of the particle size of the debris, the coarseness index (CI) will be defined, suitably revisited for this study compared to that originally proposed by Roxborough and Rispin (1973) and employed in several other studies (e.g. McFeat-Smith and Fowell, 1977; Altindag, 2003; Tuncdemir et al., 2008; Balci, 2009; Abu Bakar et al., 2014).

1. The site under study

1.1 General information

The site under investigation is the *Maddalena* exploratory tunnel: this is one of the four preliminary works to the construction of the new Turin-Lyon link, which will extend for 57 km between Susa, in Piedmont (Italy) and Saint-Jean-de-Maurienne, in Savoy (France). The *Maddalena* exploratory

tunnel, having a length of about 7.5 km and 6.3 m in diameter, is excavated, except for the first 200 m approximately, by means of an open TBM; this solution was adopted due to the geognostic nature of the tunnel, and allowed by the conditions of the rock mass. It has in the first instance the function of deepening the knowledge on the geological and geomechanical characteristics of the rock mass, together with the objective of verifying the performance of the excavation technique adopted; secondly, it will be used as the service tunnel when the new Turin-Lyon link will be operational.

1.2 Geological context

The tunnel crosses, along its path, two main metamorphic units: the *Ambin* and the *Clarea* Complex. The geological context is shown in Figure 1. After the first 200 meters, characterized by Quaternary deposits and Piedmont Zone Units (calcschists, marbles, cargneules along a main detachment zones), the tunnel crosses the *Ambin* Complex (AMC), substantially made by aplitic gneiss, for about 1 km. It is then encountered a contact zone (AMD), which extends for a few hundred meters between the two main units, composed of alternations of quartz-mica schist and gneiss (albite). The remaining 6 km cross the *Clarea* Complex (CLR), substantially characterized by Clarea-mica schist: the results proposed in this study refer to samples taken within this Complex, which has a RMR ranging from 41 and 80. The tunnel crosses areas with low average permeability, which develop when matching sub-vertical fault zones.

1.3 TBM characteristics

The machine employed is a single gripper open HP Robbins TBM (main technical characteristics summarized in Table 1) having a diameter of 6.3 m and an overall length of 240 m.

The transport of the excavated material takes place by means of a conveyor belt, which discharges it outside the tunnel in a portion of the yard used as a storage area.

1.4 TBM data

The recording of the TBM data is performed by an automatic detection system and data logging that can read, view and collect the most significant excavation parameters, such as: cutterhead torque, total thrust, cutterhead rotational speed, rate of penetration, gripper pressure, thrust cylinder advancement, TBM excavation state and tunnel chainage. The collected data are available for downloading in real time through a server.

In order to optimize the study of the TBM performance, a set of Matlab codes/scripts for the machine data management were specially developed. Such codes allow to:

- create a database that collects both the machine data and the related geomechanical data of the rock mass examined;
- to get the machine parameters, characteristic of the excavation efficiency, derived from those recorded by the TBM (Balci, 2009; Hassanpour et al., 2011; Bilgin et al., 2014).
- to filter the data as a function of the study to be carried out: for instance, to assess the machine performance in actual excavation conditions, or to evaluate the downtimes;
- to consult in an optimal way the data within a given range of the chainage, both in analytical form and on a set of graphics.

The derived parameters of the TBM that are presented in this study were obtained by the following equations:

$$Fn = \frac{FT}{N_{cutter}} \qquad FPI = \frac{Fn}{ROP} \qquad SE = \frac{2 \cdot \pi \cdot RPM \cdot T}{PR} \qquad (1)$$

where:

- Fn : mean force on a single cutter [kN/disc];
- FT : total cutterhead thrust [kN];
- N_{cutter}: number of cutters;
- FPI: field penetration index [kN/disc/mm/rev];
- ROP: rate of penetration [mm/rev];

- SE: field specific energy [MJ/m^3];
- RPM: rotational speed [rev/min];
- T: cutterhead torque [MN·m];
- PR: penetration rate [m^3/min].

1.5 Rock mass data

The investigation and monitoring of rock mass during the tunnel excavation include extensive tests both on site and in the laboratory. This study refers to the results obtained by geological/geomechanical surveys carried out on a daily basis (about every 10 m of excavation) on the tunnel walls, in accordance with the ISRM (1978) suggestions. In particular, the following rock-mass parameters will be analyzed: Rock Mass Rating RMR (Bieniawski, 1989); Geological Strength Index GSI (Hoek et al., 1998); joint spacing and Uniaxial Compression Strength UCS obtained from the Point Load Test following the suggestions of Broch & Franklin (1972); it should be noticed that the UCS determined during the crossing of *Clarea* mica-schists corresponds to the average between the value obtained perpendicular to the schistosity and that parallel to it.

2. Methodology

2.1 *Split Desktop* software

Split Desktop is an image processing software primarily used in the mining and mineral industry to estimate the size distribution of rock fragments in the various stages of processing. It is able, starting from one or more photographic images of rock fragments, to determine the 3D volumes of fragments by the image processing and appropriate statistical calculations (Kemeny, 1994).
Particularly, the software, through an almost entirely automated process, outlines the rock fragments contained in the image, in order to determine the contours and consequently the 2D dimensions. From these results, by means of suitable algorithms, the 3D sizes of the fragments are evaluated, which, compared with those of a series of virtual sieves defined by the user, allow the determination of the particle size distribution of the rock fragments analyzed.
It is noteworthy that, during the processing phase, a dimension called "cutoff" will be defined, below which the software is no longer able to recognize the fragments of rock, because they are too small compared to the image resolution. The particle size distribution of the material recognized with dimensions greater than the cutoff, is determined by the direct processing of the surfaces outlined on the image, from which the volumes of the fragments are determined; as for the portions whose dimensions are lower than the cutoff, the software refers to specific statistical distribution relations attributed to the finer material.

2.2 Sampling

By means of a wheel loader, about 3 m^3 of debris discharged from the conveyor belt are picked up on one of the storage heaps outside the tunnel; it is important to refer to the newly deposited material, so as to trace the instant when it was excavated and, therefore, the relative chainage of the tunnel. The sample taken is then moved to an adjacent place, where it can be analyzed without interfering with the other activities of the stope; the material is spread so as to create a flattened surface, to optimize the photographic analysis result, by reducing the geometric distortion. At this point, by means of a high-resolution camera, 9 photographs are taken to the portion of debris analyzed in the following way (Figure 2):

- 1 photo of the muck-pile, to get an overall picture;
- the muck-pile is virtually divided into 4 parts;
- for each part of it, 2 photos are taken: one closer (horizontal length of the image of about 50 cm), and the other one more distant (horizontal length of 1-1.5 m): referring to different scales, it is in fact possible to keep the reliability of the analysis on a broader range of the fragments size;
- before taking each photo, elements of known size are positioned: they are needed, during the image processing, for the allocation of scaling; in the analysis here presented, two

rubber balls with 6 cm diameter were used.

At this point the material can be relocated in the original muck-pile and the sampling phase has been completed; to be noticed that this step can be performed in about 10 minutes.

2.3 Image processing

In order to achieve a good compromise between representativeness of the sample and analysis times, the processing phase affects only two of the four parts into which the sample was divided: reference is made to two opposite portions, according to the principle of quartering (Gertsch, 2000). For each sample, 4 pictures are then processed, considering that 2 photos for each portion of the sample were taken: large-scale and small scale. Each photo is processed in the following way:

- image loading on the software;
- automatic delineation of individual rock fragments on the image;
- definition of the scale, by means of the reference elements on the image;
- manual modification of the automatic delineation performed: this is necessary if significant inaccuracies are found in the phase of delineation of the fragments performed by the software; it is, however, a good rule to always perform a manual editing, in order to optimize the processing result;
- definition of the "fines factor", namely the amount of the fines present in the portions of the image that the software is not able to sketch. In the case examined, the "fines factor" was chosen equal to 10% by applying the recommended guidelines from the software developers: reference was made to the characteristics of the debris found on average, and the value was kept constant for all images analyzed, so as to excellently perform the comparison between different samples from the same site.

The overall duration of the processing phase varies substantially according to the duration of the manual editing phase, which depends on user's discretion, according to the degree of precision to be achieved. In the present case, it was obtained an optimal processing level employing approximately 20-30 minutes for each image.

At this point, the software is able to return the grain size analysis results, both graphically and analytically. A particularly advantageous aspect of the photographic approach, compared to that by sieving, is the result customization: it is in fact possible to choose the size of the virtual sieves used for the evaluation of the particle size as a function of the aims of the study. In Figure 3 some of the main processing stages by *Split Desktop* are depicted.

As previously mentioned, for the fragments whose size is greater than the cut-off, *Split Desktop* performs a direct evaluation based on the graphic processing of the image; as for the finer fragments, the results are obtained by means of a statistical estimation. For these reasons, in order to refer only to the results derived from the direct evaluation of the software, in this study it was decided to refer to the portion of the grain size distribution above the cut-off (about 10 mm for the performed analysis).

2.4 Determination of the coarseness index (CI)

The coarseness index (CI) is a dimensionless number which provides a comparative measure of the size and distribution of the debris produced (McFeat-Smith and Fowell, 1977). It was originally calculated by Roxborough and Rispin (1973) as the sum of cumulative weight percentages retained on each sieve used. In this study, the CI was calculated as shown in Table 2.

Compared to the original version, the cumulative percentage refers to the volume of the fragments obtained from the analytical results provided by *Split Desktop*, and the reference size of sieves have been revised in accordance with the choice to go into detail for the only coarse portion of the debris analyzed.

2.5 Data processing

To compare the results obtained by photographic analysis with those obtained by other investigations it is necessary to classify the debris analyzed as a function of the chainage where it was produced. The definition of the chainage passes through the determination of the time displayed by the TBM, in accordance with the following relationship:

$$TBM_{time} = Image_{time} \pm \Delta time_{TBM-Image} - Belt_{time} - Loader_{time}$$

where:

- TBM_{time} is the time shown by the TBM clock, to which refer to assess the machine data;
- $Image_{time}$ is the time where the first picture of the tested muck-pile was taken (time displayed by the camera);
- $\Delta time_{TBM-Image}$ is the discrepancy between the clock of the TBM, and that of the camera;
- $Belt_{time}$ is the time taken by the debris to be transported on the conveyor belt from the excavation face to the outside muck-pile, according to the chainage reached and to the speed of the conveyor belt;
- $Loader_{time}$ is the time required by the wheel loader to load and to arrange the material.

Once defined the TBM_{time}, it's possible to go back to the machine data on a range of ± 10 minutes, in order to optimally assess the variability of parameters and to take account of any discrepancies with the estimation made, such as stops, or slopes and jumps of the conveyor belt (example in figure 4).

3. Results

Table 3 shows the results obtained from 8 debris samples taken while crossing the *Clarea* Complex (see Figure 1); specifically, the results of the particle size distribution are shown together with the related TBM data and the rock mass parameters.

The results on the debris also include three parameters expressing the average characteristics of the coarse portion of the debris analyzed: the D_{50}, also known as the median diameter or the medium value of the particle size distribution, that expresses the value of the particle diameter at 50% in the cumulative distribution; the D_{max}, that the software associates to 99.95% in the cumulative distribution, and the ratio D_{75}/D_{50}. High values of D_{50}, as well as CI, correspond to a larger average particle size and consequently to a lower comminution; the ratio D_{75}/D_{50} is rather indicative of the degree of uniformity of particle size distribution. Data on the rock mass characteristics refer, as specified above, to the results of geomechanical surveys carried out in the tunnel section where the analyzed debris was taken. It is also shown that the values of the pairs A-B, C-D and E-F belong to samples taken during the same day at a distance of several hours; for this reason, being known the frequency of geomechanical survey which, as said before, is on a daily basis, the mentioned pairs of samples show the same values of the rock mass parameters.

3.1 Grain size distribution

The particle size distribution of the coarse portion of the samples analyzed is given in Figure 5: it shows how the samples E and F differ considerably from the other samples tested, presenting a significantly finer particle size, detectable in the CI values, as well as in the D_{50}, D_{max} values, noticeably smaller.

All samples show rather a fairly wide distribution in the range 10-200 mm: this can be highlighted, in addition to the trend of particle size distribution, by the values of D_{75}/D_{50} ratio, which all fall within a range between 1.6 and 2; this condition shows that, for the samples tested, there is no relationship between this ratio and the parameters analyzed.

3.2 TBM parameters vs. grain size distribution of the debris

Hereinafter the trends of the machine parameters which express the performance of the TBM depending on the coarseness index (CI) are shown. Among these, it is noticeable the correlation between the specific energy, indicative of the excavation efficiency, and the CI: from the mechanical rock boring theory it is in fact known that, for a given rock, a larger particles size involves a lower specific energy consumption (Ozdemir, 1992). Figure 6 shows how the inverse trend between SE and CI, highlighted in several studies (e.g. Roxborough and Rispin, 1973; Tuncdemir et al., 2008; Abu Bakar et al., 2014), is also noticed by the experimental results obtained in this research.

Figure 7 shows the values of the field penetration index (FPI) as a function of the CI. The downward trend of FPI when CI increases is observable. Keeping in mind that low values of FPI correspond to a greater aptitude of the rock mass to be penetrated, it is observable that, in the site under examination, a greater comminution is obtained in correspondence of more easily penetrable rock portions.

Figure 8 shows a reverse trend also between the Normal Cutter Force (Fn) and CI: it means that the particle size decreases when the force applied to the cutterhead increases. This is in contrast to what usually takes place in intact rock conditions, where an increase of the force applied to the disk tools entails an increase of the penetration, which results in a larger average size of the rock chips produced. The relationship between CI and ROP shown by Roxborough & Rispin (1973) in the intact rock is in fact not observed in the case examined: in Figure 9 it can be seen that, in the rock type tested, the CI shows a series of quite dispersed values with respect to ROP. This condition is mainly attributable to the fracturing of the rock mass examined. Several studies show, in fact, that both the rate of penetration and the particle size distribution of the debris are strongly influenced by the rock mass characteristics and especially by its fracturing. Nelson (1993), by means of on-site results, and Gong et al. (2006), through 2D numerical models, show that the joint spacing respectively affects the FPI and the ROP. Balci (2009), on the basis of on-site results points out that, in contrast to the theory and laboratory tests on intact rock (e.g. Roxborough & Phillips, 1975), the thrust applied to the cutterhead and the ROP do not show any relationship; this condition, which can also be found in the values of Fn and ROP obtained in the site under examination (Figure 10), can be attributed to the effect of frictional forces induced on the cutterhead by the collapse of some rock mass portions at the crown and the face of the tunnel.

Abu Bakar et al. (2014) show that both the production rate and the chip size can greatly differ from the results obtained in the laboratory. In particular, the presence of fractures within the rock mass seems to have different effects on the CI: on the one hand, in fact, the fracturing of the rock mass may induce, compared to the intact rock conditions, a decrease of the CI because of the greater presence of fines, caused by the overcrushing in front of the cutterhead (Balci, 2009); on the other hand, on the contrary, the fracturing at the excavation face can cause the displacement and the entry in the binders of rock blocks bigger than those required by the normal process of chip formation (Farrokh and Rostami, 2008).

Figure 11 shows, finally, that a significant trend between the torque and the CI is not noticeable.

3.3 Grain size distribution of debris vs. rock mass parameters

Figure 12 shows that the relationship between the CI and RMR is not noticeable; this condition, which can also be observed between CI and GSI (Figure 13), shows how the geomechanical classifications used may be unable to establish a clear relationship with the degree of comminution of the debris produced. In Figure 14, it is shown the downward trend of CI when UCS grows. Referring to the values given in Table 3, it can be noticed that the particles size does not show, in the rock mass portion examined, a clear relationship with the joint spacing; this result seems to confirm what was previously discussed: CI can take different values depending on the presence of fractures in the rock mass and therefore cannot directly be correlated to the joint spacing.

Conclusions

Particle size distribution of the debris produced by TBM's excavation, as well as determining the possible reuse of the material (Gertsch et al., 2000), can give important information both on the performance of the excavation (Roxborough and Rispin, 1973 Tuncdemir et al, 2008) and the rock mass characteristics (Balci, 2009, Abu Bakar et al, 2014). The determination on site of the particle size by sieving in a systematic way is not however easy to implement in terms of time and costs. The study here presented has provided a methodology, based on photographic analysis, which allows the determination, in a fast and economical way, without interfering with the excavation cycle, of the particle size distribution of the coarse portion of the debris produced. The results obtained from the analysis of 8 samples of debris, collected during the crossing of a lithological unit predominantly consisting of mica-schists, were compared to the TBM performance and the rock mass characteristics. The results obtained have first shown how the coarseness index (CI) follows a reverse trend with respect to the specific energy, according to the theory and to various investigations both on laboratory and on site. The comparison between the FPI and CI shows that, when the attitude of the rock mass to be penetrated increases, there is also an increase in the size of the fragments. Instead of what occurs in the intact rock, it has been seen how, for the same lithotype crossed, the increase of the force applied to the cutterhead leads to an increase of the comminution of the material; moreover, it has not been found a consistent relationship between ROP and CI, as evidenced by Roxborough and Rispin (1973) from laboratory tests. This condition is likely due to the effect that the fracturing of the rock mass has on the ROP, as shown by several studies (e.g. Gong et al., 2006; Abu Bakar et al., 2014).

The results have also shown that the size of the fragments is influenced by the rock mass characteristics but, in the examined site, a clear relationship between the parameters has not been found. In particular, it was observed that CI does not show a consistent relationship with RMR and GSI; this condition is mainly due to the nature of those geomechanical classifications, which take into account various parameters of the rock mass that influence the size of the debris with different effects: on one hand, in fact, the influence of the characteristics of intact rock, such as the UCS, cannot be disregarded (UCS exhibited a slightly decreasing trend with respect to CI in this site); on the other side, there are the conditions of the rock mass, as the joint spacing, that have not shown a significant relationship with the CI; this confirms that an increase of the rock mass fracturing may involve a dual effect on the size of the debris: a decrease of the CI, because of the greater presence of fine caused by the over-crushing in front of the cutterhead, but also an increase of the CI, due to the detachment of large fragments of rock at the excavation face.

References

Abu Bakar, M.Z., Gertsch, L., Rostami, J., 2014. Evaluation of fragments from disc cutting of dry and saturated sandstone. Rock Mech. Rock Eng. 47 (5), 1891–1903.

Altindag, R., 2003. Estimation of penetration rate in percussive drilling by means of coarseness index and mean particle size. Rock. Mech. Rock. Eng. 36(4), 323–332.

Balci, C., 2009. Correlation of rock cutting tests with field performance of a TBM in a highly fractured rock formation: a case study in Kozyatagi-Kadikoy Metro Tunnel, Turkey. Tunn. Undergr. Space Technol. 24, 423-435.

Bieniawski, Z.T. 1989. Engineering rock mass classifications. John Wiley & Sons, New York.

Bilgin, N., Copur, H., Balci, C., 2014. Mechanical Excavation in Mining and Civil Industries. CRC Press, Taylor and Francis Group, p. 366, ISBN-13: 978-1466584747.

Broch, E., Franklin, J.A., 1972. The point-load strength test. Int. J. Rock Mech. Min. Sci. 9, 669-697.

Bruland, A., 1998. Hard Rock Tunnel Boring, Performance Data and Back-Mapping, vol. 6. University of Sciences and Technology of Trondheim (NTNU) – Project report 1E-98.

Farrokh, E., Rostami, J., 2008. Correlation of Tunnel Convergence with TBM Operational Parameters and Chip Size in the Ghomroud Tunnel, Iran. Tunn. Undergr. Space Technol. 23, 700-710.

Gertsch, L., Fjeld, A., Nilsen, B., Gertsch, R., 2000. Use of TBM muck as construction material. Tunn. Undergr. Space Technol. 15(4), 379-402.

Gong, Q.M., Jiao, Y.Y., Zhao, J., 2006. Numerical modelling of the effects of joint spacing on rock fragmentation by TBM cutters. Tunn. Undergr. Space Technol. 21 (1), 46–55.

Hassanpour, J., Rostami, J., Zhao, J., 2011. A new hard rock TBM performance prediction model for project planning. Tunn. Undergr. Space Technol. 26: 595-603.

Hoek, E., Marinos P., Benissi M., 1998. Applicability of the geological strength index (GSI) classification for weak and sheared rock masses – the case of the Athens schist formation. Bull Eng Geol Env 57(2):151-160

ISRM, 1978. Suggested Methods for the Quantitative Description of Discontinuities in Rock Masses. Rock Characterisation Testing and Monitoring, Pergamon, Ed. E.T. Brown, 1981.

Kemeny, J., 1994. A practical technique for determining the size distribution of blasted benches, waste dumps, and heap-leach sites. Mining Engineering, 46(11): 1281-1284.

McFeat-Smith, I., Fowell, R.J., 1977. Correlation of rock properties and the cutting performance of tunnelling machines. Proceedings of a Conference on Rock Engineering. The University of Newcastle Upon Tyne, pp. 581-602.

Nelson, P.P., 1993. TBM performance analysis with reference to rock properties. In: Hudson, J.A. (Ed.), Comprehensive Rock Engineering. Pergamon Press, Oxford, pp. 261–292.

Ozdemir, L., 1992. Mechanical excavation techniques in underground construction. Short Course Notebook, vol. 1. Istanbul Technical University.

Parisi, M.E., Farinetti, A., Gilli, P., Brino, L., 2015. First results from the excavation of the Lyon - Turin Maddalena Exploratory Tunnel. ITA WTC Congress and 41st General Assembly; Proc. intern. Symp., May 22-28, Dubrovnik, Croatia, 0-11.

Roxborough, F.F., Rispin, A., 1973. The mechanical cutting characteristics of the lower chalk. Tunn. Tunn. 5: 45-67.

Roxborough, F.F., Phillips, H.R., 1975. Rock excavation by disc cutter. Int. J. Rock Mech. Min. Sci. Geomech. Abstr. 12, 361–366.

Rispoli, A., Ferrero, A.M., Cardu, M., Brino, L., Farinetti, A., 2016. Hard rock TBM performance: preliminary study based on an exploratory tunnel in the Alps. Rock Mechanics and Rock Engineering: From the Past to the Future – Ulusay et al. (Eds), 2016, Taylor & Francis Group, London, 469-474, ISBN 978-1-138-03265-1.

Tuncdemir, H., Bilgin, N., Copur, H., Balci, C., 2008. Control of rock cutting efficiency by muck size. Int. J. Rock Mech. Min .Sci. 45 (2), 278–288.

BS EN 933-1, 2012. Tests for geometrical properties of aggregates. Determination of particle size distribution. Sieving method. BSI Standards Publication. February 2012, ISBN 978 0 580 74432 7, 0-22.

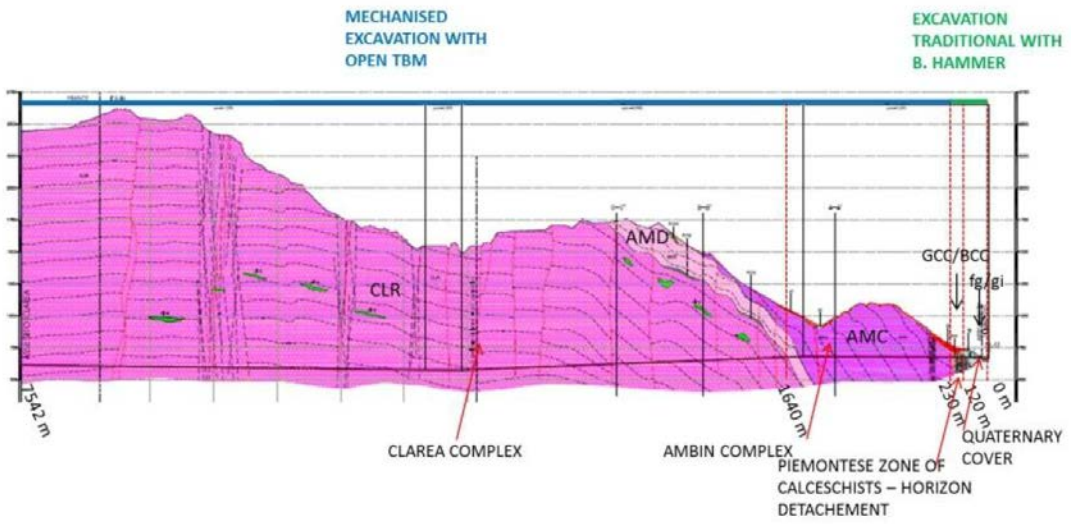

Figure 1. Geological context of the Maddalena exploratory tunnel (Parisi et al., 2015)

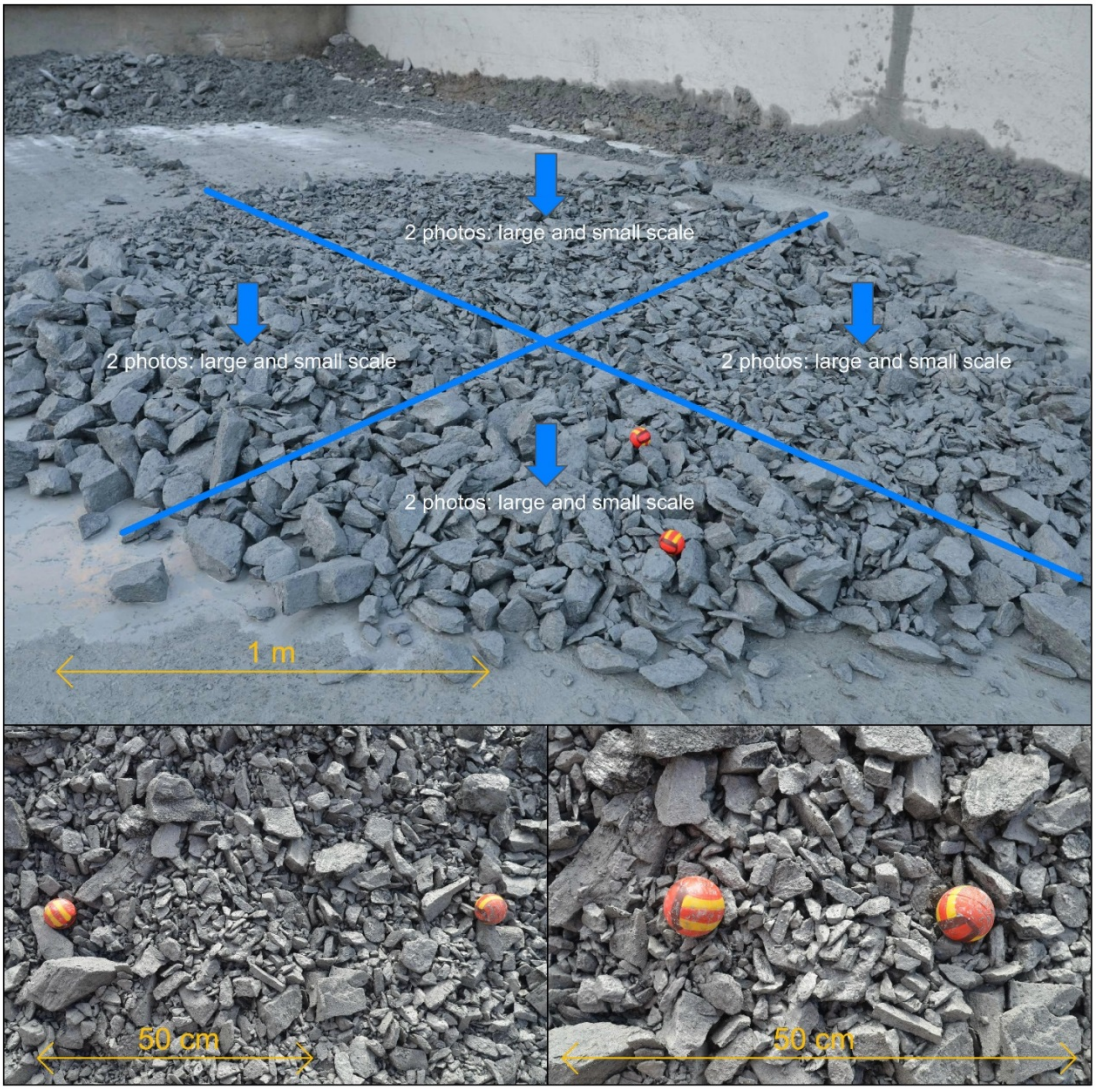

Figure 2. Above: subdivision of the muck-pile into 4 parts; for each one of them two photos are taken at different scales; below: 2 photos of the same portion of muck-pile taken at different scales, respectively large-scale (left) and small scale (right).

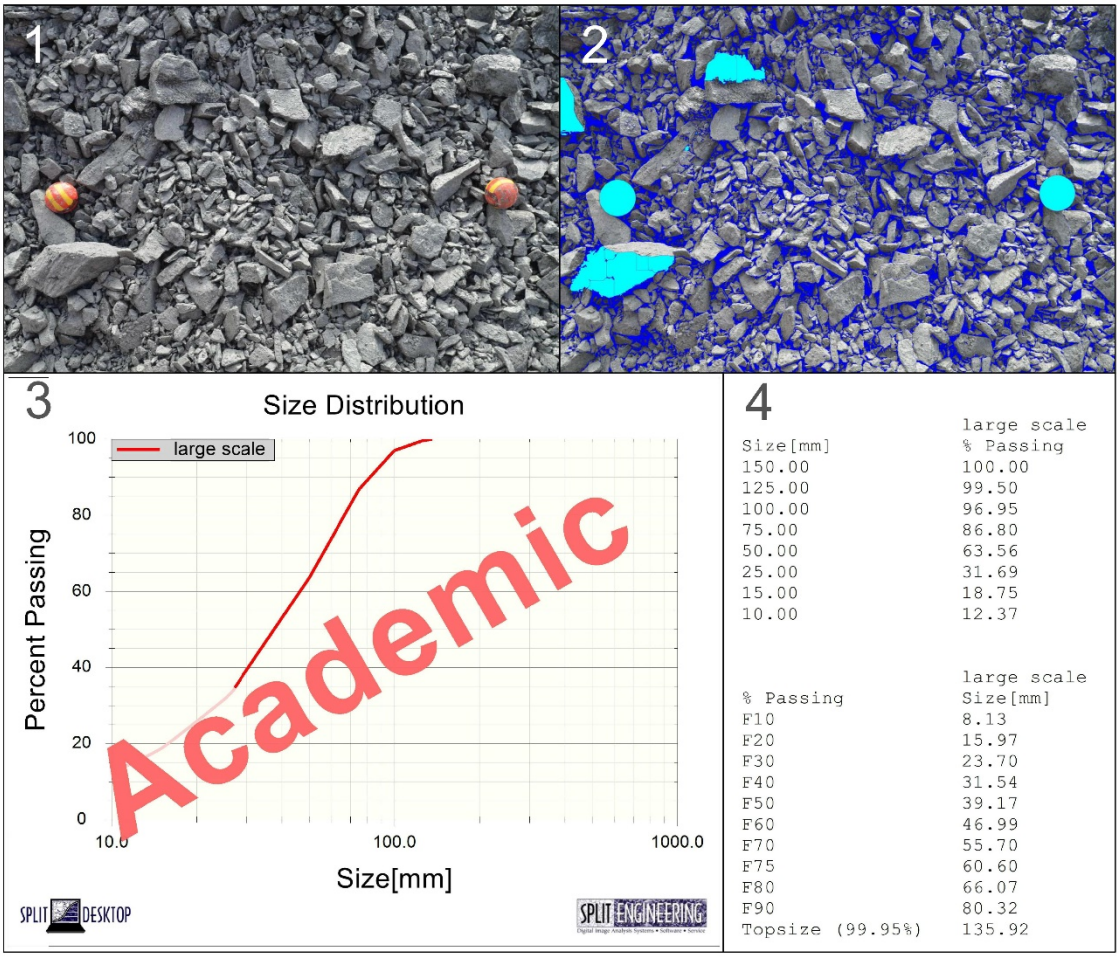

Figure 3. Some processing steps using the Split desktop software: 1) loaded image, 2) outlined and scaled image, 3) graphical restitution of the result, 4) analytical restitution of the result

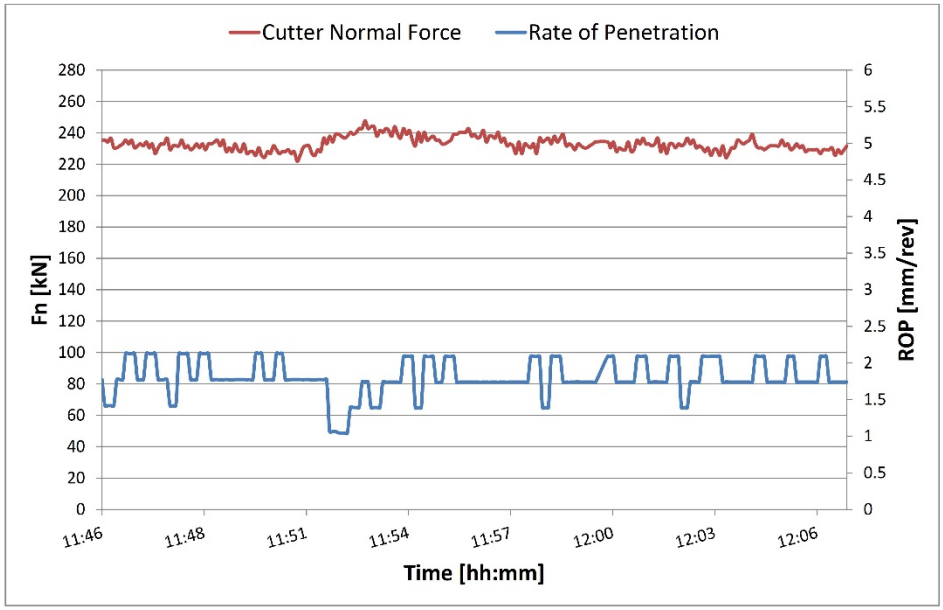

Figure 4. Example of evaluation of the Cutter Normal Force (Fn) and Rate of Penetration (ROP) with TBM_{time} estimated at around 11:56 hours; the time scale covers a range of ± 10 minutes.

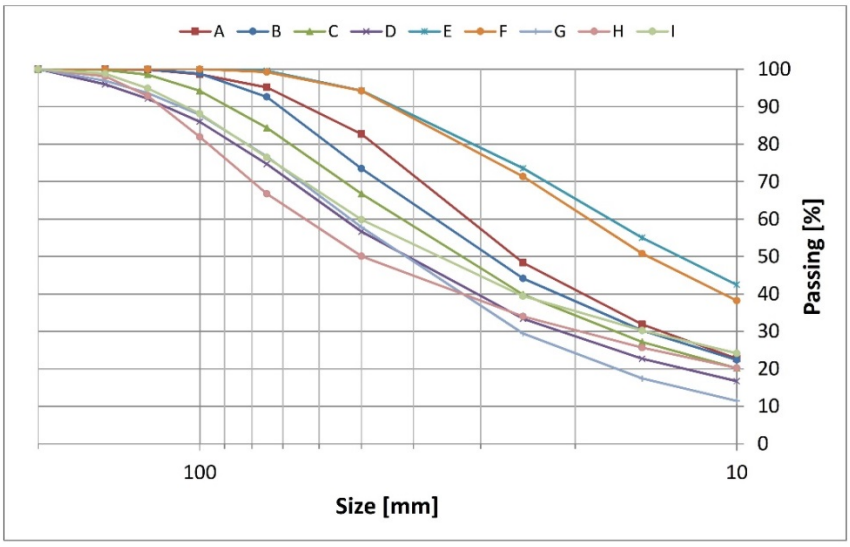

Figure 5. Grain size distribution of the 8 samples analyzed

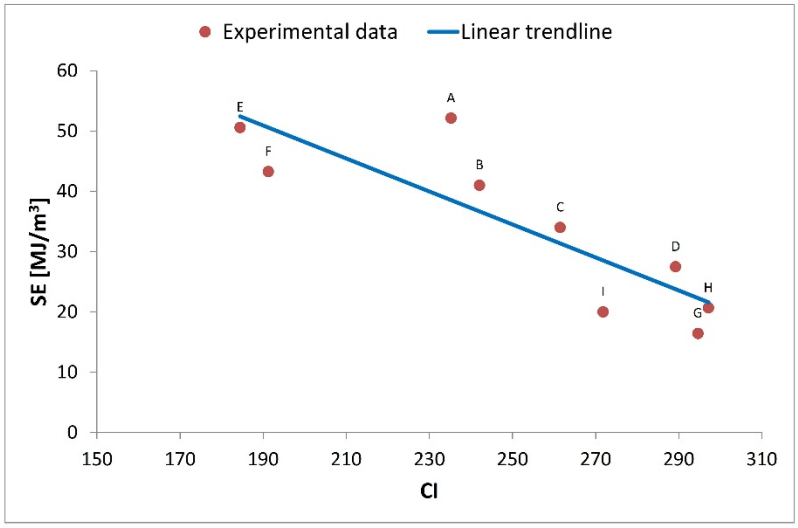

Figure 6. Field Specific Energy (SE) vs. Coarseness Index (CI). Linear trendline: $SE = -0.2737 \cdot CI + 102.91$*;* $R^2 = 0.734$

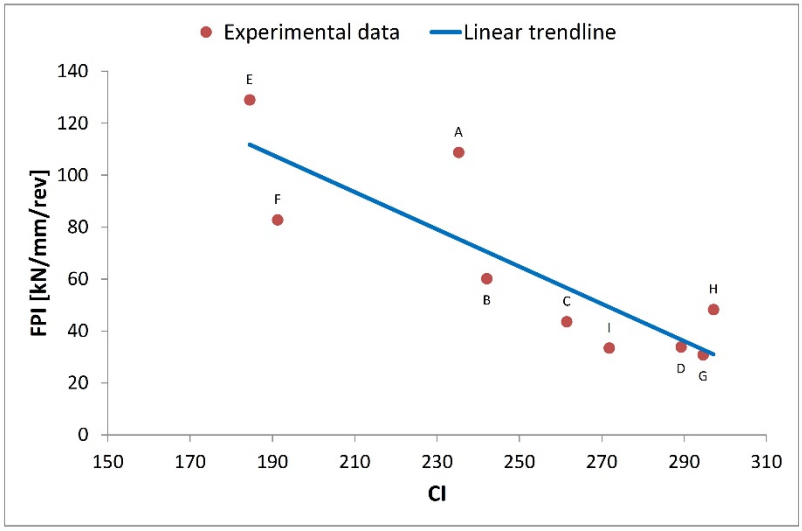

Figure 7. Field Penetration Index (FPI) vs. Coarseness Index (CI). Linear trendline: $FPI = -0.7168 \cdot CI + 244$*;* $R^2 = 0.723$

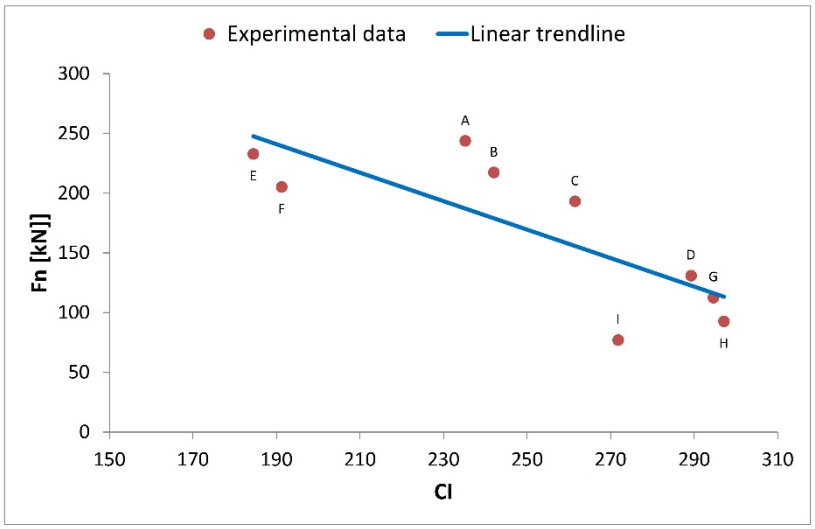

Figure 8. Normal Cutter Force (Fn) vs. Coarseness Index (CI). Linear trendline: $Fn = -1.1909 \cdot CI + 467.19$*;* $R^2 = 0.622$

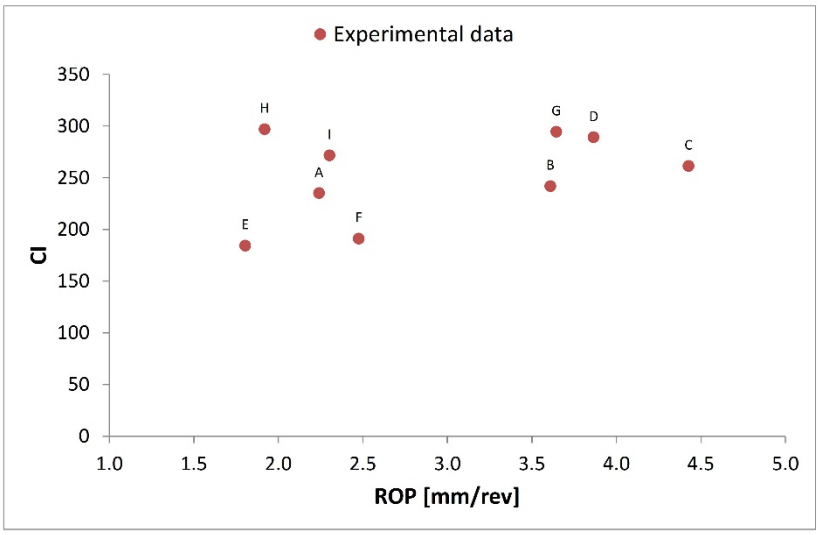

Figure 9. Coarseness Index (CI) vs. Rate of Penetration (ROP)

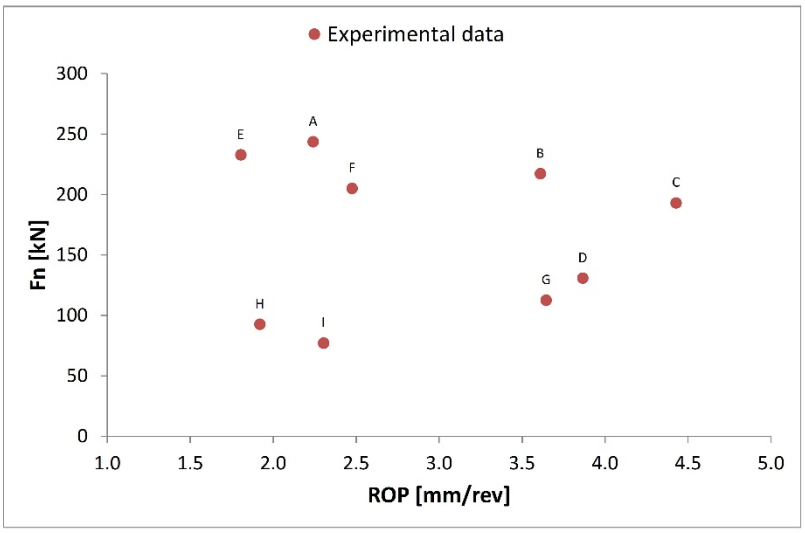

Figure 10. Normal Cutter Force (Fn) vs. Rate of Penetration (ROP)

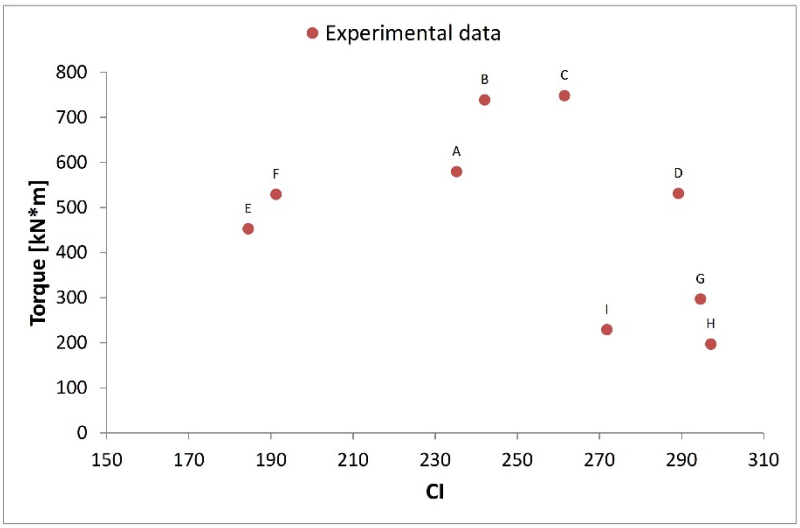

Figure11. Torque (Torque) vs. Coarseness Index (CI)

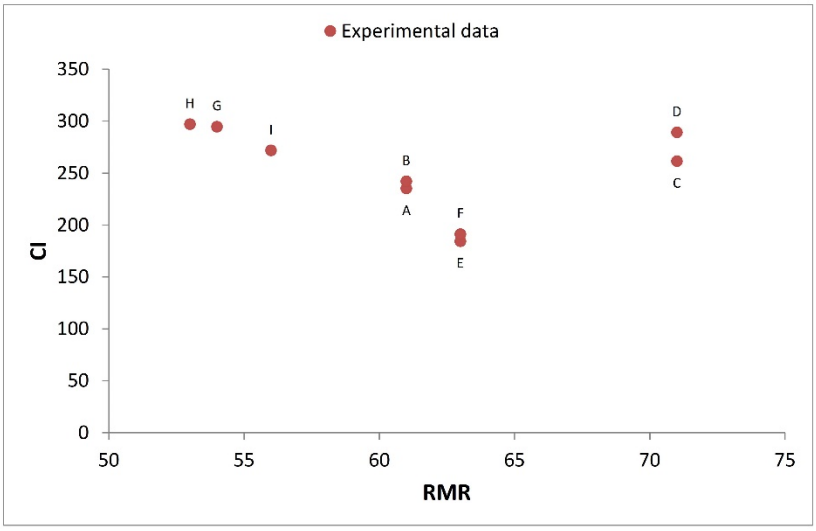

Figure 12. Coarseness Index (CI) vs. RMR

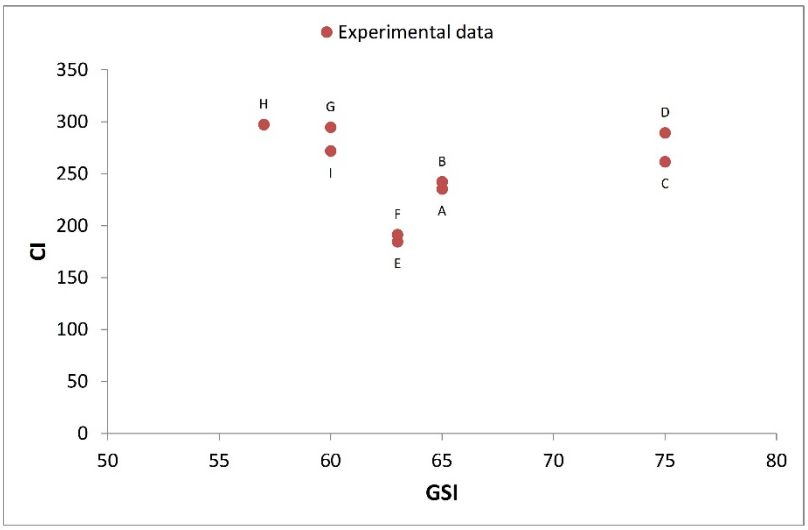

Figure 13. Coarseness Index (CI) vs. GSI

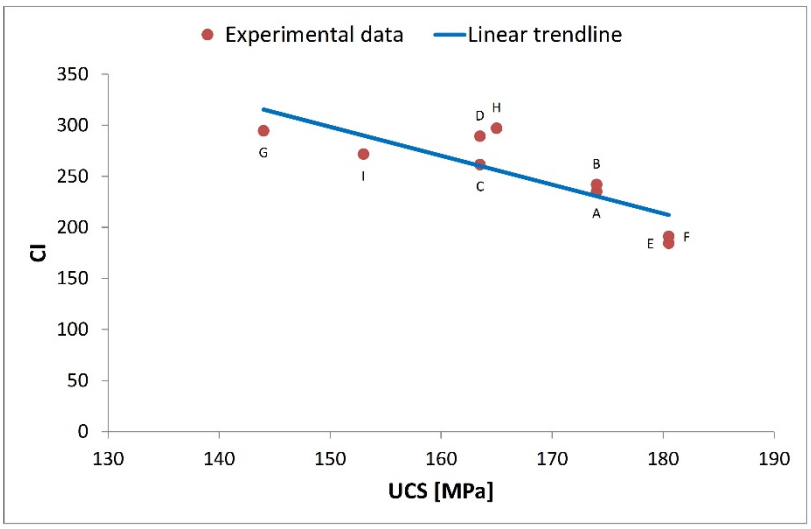

Figure 14. Coarseness Index (CI) vs. Uniaxial Compression Strength (UCS). Linear trendline: $CI = -2.8275 \cdot UCS + 722.53$; $R^2 = 0.676$

Table 1 – Technical characteristic of the TBM

Cutterhead thrust – recommended	12,800 kN
Maximum machine thrust	13,700 kN
Cutterhead power	2,202.8 kW
Cutterhead torque	2,082.9 kN·m
Cutterhead speed	0-10.8 rpm
Number of main thrust cylinder	4
Thrust cylinder stroke	1,800 mm
Hydraulic system power	111.9 kW
Gripper total force	36,400 kN
Numbers of disc cutters	43
Disc cutters size	17” (431.8 mm)

Table 2 – Example of coarseness index (CI) calculation

Size fraction [mm]	Passing [%]	Cumulative passing [%]
+ 100	1.4	1.4
- 100 +75	3.5	4.9
-75 +25	46.8	51.7
-25 +10	25.6	77.3
-10	22.7	100.0
Total	100.00	CI =235.2

Table 3. Particle size analysis results and parameters related to the TBM and the rock mass on 8 samples taken while crossing the *Clarea* Complex in *Maddalena* exploratory tunnel. TBM data: Fn: normal force applied on average on each cutter; RPM: rotational speed of the cutterhead; ROP: rate of penetration; FPI: field penetration index; Torque: cutterhead torque; SE: field specific energy.

Sample reference			A	B	C	D	E	F	G	H	I
Sieve size [mm]	200	Passing [%]	100.0	100.0	100.0	100.0	100.0	100.0	100.0	100.0	100.0
	150		100.0	100.0	99.8	96.0	100.0	100.0	96.9	98.0	98.8
	125		99.9	100.0	98.5	92.1	100.0	100.0	93.6	92.8	94.9
	100		98.6	98.8	94.2	86.0	100.0	100.0	87.8	81.9	88.1
	75		95.1	92.6	84.3	74.7	99.6	99.2	76.7	66.7	76.5
	50		82.7	73.4	66.7	56.6	94.3	94.2	57.8	50.1	59.9
	25		48.3	44.1	39.8	33.4	73.6	71.3	29.4	34.0	39.4
	15		31.9	30.2	27.2	22.7	55.0	50.8	17.4	25.7	30.3
	10		22.7	22.4	20.2	16.7	42.4	38.2	11.5	20.3	24.2
Size fraction [mm]	+100	Cumulative passing [%]	1.4	1.2	5.8	14.0	0.0	0.0	12.2	18.1	11.9
	-100 +75		4.9	7.4	15.7	25.3	0.4	0.8	23.3	33.3	23.5
	-75 +25		51.7	55.9	60.2	66.6	26.5	28.7	70.6	66.0	60.6
	-25 +10		77.3	77.6	79.8	83.3	57.6	61.8	88.5	79.8	75.8
	-10		100.0	100.0	100.0	100.0	100.0	100.0	100.0	100.0	100.0
Muck parameters		CI	235.2	242.1	261.5	289.2	184.5	191.2	294.6	297.1	271.8
		D_{50} [mm]	26.0	29.6	33.5	42.4	12.9	14.7	42.1	49.9	37.3
		D_{75}/D_{50}	1.6	1.7	1.8	1.8	2.0	1.9	1.7	1.8	1.9
		D_{max} [mm]	126.8	114.2	164.1	189.3	80.1	95.6	196.5	175.7	165.6
TBM data		Fn [kN/cutter]	243.7	217.2	193.1	130.9	232.7	205.1	112.6	92.7	77.0
		±	7.8	16.9	16.6	14.7	4.5	26.8	6.0	15.6	11.8
		RPM [rev/min]	8.2	7.8	7.6	6.9	9.5	8.8	5.1	8.4	4.3
		±	0.0	0.4	0.3	0.5	0.1	0.7	0.0	0.3	0.2
		ROP [mm/rev]	2.2	3.6	4.4	3.9	1.8	2.5	3.6	1.9	2.3
		±	0.4	0.8	0.7	0.8	0.2	0.7	0.5	0.6	1.0
		FPI [kN/cutter/mm/rev]	108.7	60.2	43.6	33.9	129.0	82.8	30.9	48.3	33.5
		±	23.5	17.8	10.3	11.1	19.8	34.8	6.0	23.9	19.7
		Toque [kN·m]	579.8	738.9	748.4	531.5	453.0	529.6	297.0	197.2	229.2
		±	77.4	157.9	128.9	138.9	48.9	147.7	62.8	77.3	212.5
		SE [MJ/m^3]	52.2	41.0	34.0	27.5	50.6	43.3	16.4	20.7	20.0
Rock mass characteristics		Lithology	Mica-schist	Mica-schist	Mica-schist	Mica-schist	Mica-schist	Mica-schist	Mica-schist	Mica-schist	Mica-schist
		RMR	61	61	71	71	63	63	54	53	56
		GSI	65	65	75	75	63	63	60	57	60
		Joint Spacing [cm]	50-100	50 - 100	100-200	100-200	20-50	20-50	20-50	50-100	50-100
		UCS [MPa]	174	174	164	164	181	181	144	165	153